Clinical Cancer

Research

Characterization of a novel androgen-sensitive, prostate-specific antigen-producing prostatic carcinoma xenograft: LuCaP 23.

W J Ellis, R L Vessella, K R Buhler, et al.

Updated Version	Access the most recent version of this article at: http://clincancerres.aacrjournals.org/content/2/6/1039

Citing Articles	This article has been cited by 19 HighWire-hosted articles. Access the articles at: http://clincancerres.aacrjournals.org/content/2/6/1039#related-urls

E-mail alerts	Sign up to receive free email-alerts related to this article or journal.
Reprints and Subscriptions	To order reprints of this article or to subscribe to the journal, contact the AACR Publications Department at pubs@aacr.org.
Permissions	To request permission to re-use all or part of this article, contact the AACR Publications Department at permissions@aacr.org.

Characterization of a Novel Androgen-sensitive, Prostate-specific Antigen-producing Prostatic Carcinoma Xenograft: LuCaP 23[1]

**William J. Ellis,[2] Robert L. Vessella,
Kent R. Buhler, Franck Bladou,
Lawrence D. True, Steven A. Bigler, Dena Curtis,
and Paul H. Lange**

Department of Urology, University of Washington, Seattle,
Washington 98195 and Section of Urology, Seattle Veterans Affairs
Medical Center, Seattle, Washington 98108

ABSTRACT

Prostatic carcinoma has proven extremely difficult to establish as cell lines or xenografts. In this article, we describe a new series of prostate cancer xenografts propagated in athymic mice, designated LuCaP 23, developed from prostate metastases harvested at autopsy shortly after death. Tumor from three separate metastatic deposits was developed into three xenograft sublines: two from lymph node metastases (LuCaP 23.1 and 23.8) and one from a liver metastasis (LuCaP 23.12). Fluorescence in situ hybridization analysis confirms the xenografts are human. Histologically, the xenografts are comprised of columnar epithelial cells arranged in a glandular pattern. Tumor doubling times range from 11 to 21 days for the three sublines. The cells secrete large amounts of prostate-specific antigen (PSA) with PSA indices of 1.27, 1.63, and 5.21 ng/ml/mm^3 for the mice bearing the LuCaP 23.1, 23.8, and 23.12 sublines, respectively. Following androgen deprivation a temporary decrease in PSA secretion and a decrease in tumor size are noted in most tumors. Eventually, the tumors become androgen independent and resume growth in castrate hosts. The degree of PSA response to castration and time to PSA nadir correlate with time to progression. Thus, unlike most existing models of prostatic carcinoma, this novel xenograft exhibits many phenotypic characteristics of clinical prostatic carcinoma, including androgen sensitivity. These properties make this xenograft an excellent model for future study.

INTRODUCTION

Carcinoma of the prostate is the most commonly diagnosed malignancy and the second leading cause of cancer-related death in American men (1). Insight into the biological behavior of this disease lags behind that of many other solid tumors. In part, this deficiency is due to the lack of adequate in vivo and in vitro models available for study, especially when compared to other common tumors such as breast, lung, and colon. At this time, only eight continuously passaged prostate cancer cell lines (2–10) and nine serially passable xenografts lines (both primary and metastatic) (9, 11–17) currently exist (summarized in Table 1).

Most of the above-mentioned xenografts and cell lines are considered inadequate models for study because they lack the multiplicity of characteristics that make for a comprehensive model, i.e., androgen sensitivity, production of PSA[3] and PAP, the ability to grow at a rate that allows timely experimentation, and growth without manipulation of hormones or growth factors. Androgen sensitivity and PSA production are two hallmarks of the prostatic phenotype, both benign and malignant, which are of clinical importance. Historically, hormonal manipulation has played a major role in the treatment of prostatic carcinoma. Today, PSA is widely used to both diagnose prostate carcinoma and monitor the effect of therapy on the disease. Thus, androgen-sensitive, PSA-producing models are desirable because they allow scientists to model clinical scenarios.

In this article, we describe a new series of prostate cancer xenografts derived from multiple metastases obtained at autopsy. These xenografts, designated the LuCaP 23 series, share many characteristics of adenocarcinoma of the prostate, and we believe they represent an excellent model for study of this disease.

MATERIALS AND METHODS

Clinical History. The donor of tissue for establishment of the LuCaP 23 series was a 63-year-old white male diagnosed with a stage D1 adenocarcinoma of the prostate with a Gleason grade of 3 + 5. He was treated with external beam radiation therapy to the pelvis. Within 6 months of completion of radiation therapy, evidence of bony metastases was discovered. The patient was initially managed with bicalutamide (Casodex) monotherapy. When evidence of disease progression was noted within a few months, bilateral orchiectomy was performed. Shortly thereafter, his disease became hormone refractory and liver metastases were detected. The patient was then treated with both Adriamycin and carboplatinum. He continued to show evidence of disease progression with extensive retroperitoneal and liver disease. The patient expired several months later with a serum PSA level of approximately 8000 ng/ml. Within 2 h of death, an autopsy utilizing aseptic technique was performed. Metastatic tumor foci from several retroperitoneal lymph nodes and the liver were harvested and returned to our laboratory for evaluation.

[2] To whom requests for reprints should be addressed, at Department of Urology, Box 356510, University of Washington, Seattle, WA 98195.

[3] The abbreviations used are: PSA, prostate-specific antigen; PAP, prostatic acid phosphatase; EGF, epidermal growth factor; DHT, di-hydro-17β-testosterone; BPH, benign prostatic hyperplasia; FISH, fluorescence in situ hybridization.

1040 LuCaP 23 Prostatic Cancer Xenograft

Table 1 Characteristics of existing prostate cancer xenografts

Name	Derived from:	Tumorigenic in mice	Androgen sensitive	PSA produced	Year derived	Reference
Established prostate cancer cell lines						
EB-33	Prostate	Yes	No	No	1974	2
DU-145	Brain	Yes	No	No	1977	3
PC-3	Vertebrae	Yes	No	No	1976	4
LNCAP	Lymph node	±	Yes	Yes	1980	5
PC-93	Prostate	No	No	No	1983	6
TSU-PR1	Lymph node	Yes	No	No	1987	7
JCA-1	Prostate	Yes	No	No	1990	8
DUPRO-1	Lymph node	Yes	No	No	1991	9
ND-1	Prostate	Yes	No	Trace	1991	10
Established prostate cancer xenografts						
PC-82	Prostate	Yes	Yes	Yes	1977	11
Honda	Testis	Yes	Yes	No	1977	12
9479	Bone	Yes	No	No	1981	13
PC-EW	Lymph node	Yes	Yes	Yes	1981	14
PC-133	Bone	Yes	No	No	1981	15
PC-135	Prostate	Yes	No	No	1982	15
PC-EG	Prostate	Yes	Yes	Yes	1984	16
TEN/12	Prostate	Yes	Yes	No	1985	17
DU5683	Lymph node	Yes	Yes	Yes	1982	9
LuCaP 23.1	Lymph node	Yes	Yes	Yes	1991	
LuCaP 23.8	Lymph node	Yes	Yes	Yes	1991	
LuCaP 23.12	Liver	Yes	Yes	Yes	1991	

Establishment of Primary Cell Lines in Vitro. Primary tissue culture was attempted for each lymph node and liver metastatic foci by placing 1–2-mm³ tissue fragments of tumor on an etched X in a 100-mm culture dish. The fragments were bathed in RPMI 1640 (BioWhittaker, Walkersville, MD) supplemented with 15% heat-inactivated fetal bovine serum (Intergen, Purchase, NY), EGF (10 ng/ml) (Collaborative Research, Bedford, MA), and DHT (0.1 ng/ml; Sigma Chemical, St. Louis, MO). In one half of the culture dishes, ascitic fluid from the patient was added to the media at a 1:4 ratio. For passage, cells were removed using 0.25% trypsin, washed with 1× PBS, and resuspended in the media described above.

Attempts were made to establish primary cell lines from xenografts (vide infra) using a variety of different protocols. The first attempt was made using the identical protocol as the primary tissues. Cellular dissociation was done both mechanically and enzymatically. Xenograft tissue was cut into small bits, passed through a cell sieve, then digested with 0.1% collagenase type IV, 0.01% hyaluronidase, and 0.002% DNase (all from Sigma Chemical) for up to 12 h at 4°C. Cells were separated from debris by layering over Ficoll-Hypaque 400 (Accurate Chemical, Westbury, NY) and centrifuging at ×100. Viable cells were plated at high densities in RPMI 1640 and DME/F12 media (BioWhittaker) both supplemented with 10% fetal bovine serum, EGF (10 ng/ml; Collaborative Research), DHT (1 × 10⁻⁸ M/ml; Sigma), bovine pituitary extract (30 μg/ml; Collaborative Research), and insulin-transferrin-selenium (20 μg/20 μg/5 ng/ml; Sigma). Other treatments of xenograft tissue include plating on collagen (Collaborative Research), fibronectin (Collaborative Research), Pronectin F (Protein Polymer Technologies, San Diego, CA), or thin-layer Matrigel (Collaborative Research)-coated tissue culture vessels. Cells were also suspended in Matrigel spaghetti using the technique of Gingrich et al. (9) and floated in the media described above.

Animals. All animal use and procedures were approved and done in accordance with the University of Washington and Seattle Veterans Affairs Animal Care Committee Guidelines. Xenografts were maintained in BALB/C-nu/nu (athymic) mice (Simonsen Laboratories, Gilroy, CA). Mice were housed in microisolator caging placed in forced HEPA-filtered air shelving units and maintained at 23.8°C room temperature, relative humidity 27–45%, on a 10-h light/14-h dark-light cycle. Picolab Irradiated Rodent Chow 20 (PMI Feeds, Inc.) and autoclaved water were provided ad libitum. s.c. tumor implantation and surgical castration were performed under ketamine/xylazine anesthesia (260.0 mg/17.6 mg/kg). Wounds were closed with 9-mm wound clips. Animals were sacrificed when tumor volume reached 1000 mm³.

Establishment of the Xenografts. Tissue from autopsy that was judged to be suitable for in vivo growth, three tissue samples from retroperitoneal lymph nodes and one from liver, was washed in 1× PBS and then soaked for 20 min in 2.5 μg/ml amphotericin (Life Technologies, Inc., Grand Island, NY) and 50 μg/ml gentamicin (Life Technologies, Inc.). Tumor bits (approximately 20–25 mm³) were then implanted s.c. in 6-week-old male athymic mice. From each metastatic foci, tumor bits were randomized among sites and animals to remove individual animal effects, giving a possible 12 sublines from the four tissues. For serial passage, xenografts were harvested at the time of animal sacrifice, cut into bits of approximately 20–25 mm³, and implanted s.c.

Determination of in Vivo Growth. Six to 8-week-old athymic mice were implanted s.c. with 20–25-mm³ tumor bits under anesthesia. The three LuCaP xenograft sublines were implanted in 10 intact male, 10 castrated male, and 10 female nude mice. Tumor volume was measured weekly as soon as the tumor was visible using microcalipers. Tumor volume was estimated using the formula of an ellipsoid (length × width ×
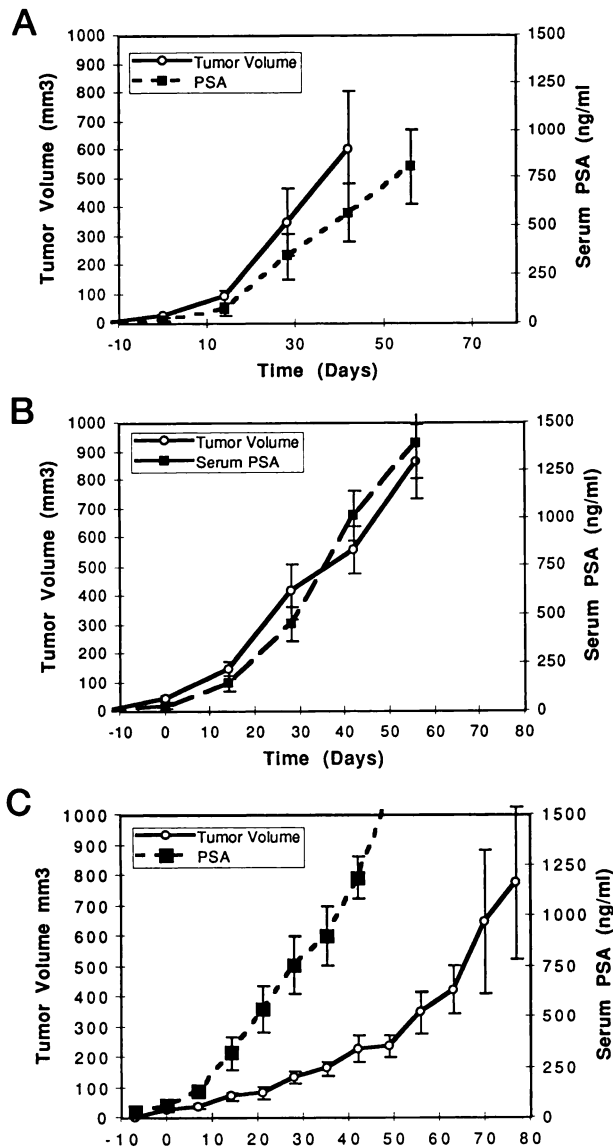
Fig. 1 Growth curves for the LuCaP 23 sublines based on tumor volume (○) and serum PSA levels (■). *A*, LuCaP 23.1; *B*, LuCaP 23.8; and *C*, LuCaP 23.12. Time 0 represents first visible tumor growth. Tumors grow in an exponential fashion with a PSA increase paralleling tumor growth. PSA production is highest in the LuCaP 23.12 xenograft, which also has the slowest growth rate.

height × 0.5236). Tumor volume doubling time was calculated during exponential growth using the formula $t[1/2] = (t_2 - t_1)/(LnV_2\text{-}LnV_1)$.

Determination of Serum PSA and PAP Concentrations. Blood samples were obtained weekly from the date of implantation by tail vein bleed into a capillary tube. Approximately 40 μl blood were collected using a 0.65-ml microcentrifuge tube and centrifuged. Fifteen to 20 μl serum were recovered and stored at −20°C until assayed. Serum PSA and PAP concentrations were determined using the automated IMx PSA immunoassay system (Abbott Laboratories, Chicago, IL) from 1:10

dilutions of 10-μl serum samples in HBSS or diluent supplied with the IMx kits.

The average PSA index, defined as the increase in serum PSA per unit of tumor volume (ng/ml/mm³), was calculated using the equation of the regression plot analysis of tumor volume against serum PSA concentration in the three xenografts. To determine the half-life of serum PSA in LuCaP 23.1 mice, PSA values were obtained before and at 2, 6, 12, 24, 36, 48, and 60 h after excision of LuCaP 23.1 tumors in seven mice. A log linear regression model was used to evaluate the half-life of serum PSA as described previously (18).

Effects of Castration. Athymic mice were implanted with tumor bits s.c. over the right scapular region. Animals with tumor volume at least 50 mm³ were castrated at 10 weeks postimplantation. Castration was performed through a transabdominal incision under anesthesia. Tumor volume and serum PSA were measured weekly after castration. PSA nadir and time to PSA nadir were compared to progression status using unpaired two-tailed *t* tests on computer software.

Histology. Five-μm paraffin-embedded tumor sections were stained with H&E to determine morphological structure and histological grading according to the method of Gleason (19). For immunohistochemical studies, 5-μm sections were deparaffinized with Histoclear II (National Diagnostics, Atlanta, GA) and rehydrated in degressive gradients of ethanol. Standard avidin/biotin-enhanced immunoperoxidase staining protocols were used to determine immunoreactivities to pertinent antibodies: the anti-PSA monoclonal antibodies 16–3A2 and 22–8A2 and the antirenal cell carcinoma/antiprostate cancer monoclonal antibody A6H, which were generated in our laboratory,[4] anti-prostate carcinoma monoclonal antibodies PD-41, TURP-27, and 7E11-C5 and anti-PAP monoclonal antibody (kindly performed by Dr. George Wright, Eastern Virginia School of Medicine, Norfolk, VA; Refs. 20–22), and a monoclonal antibody to the androgen receptor (F39.4.1; Biogenex). Nonspecific idiotype-matched monoclonal antibodies were used as negative controls. Tissue sections were blocked for endogenous peroxidases (1% H_2O_2) and biotin prior to the addition of the primary antibody. In one instance, the anti-PSA monoclonal antibody 16–3A2 was biotinylated, directly avoiding the use of a second antibody.

Electron Microscopy. Representative 5–10-mm³ fragments from throughout the tumor were fixed overnight in a mixture of 2.5% glutaraldehyde and 2% paraformaldehyde in cacodylate buffer. Tissue was rinsed in buffer and postfixed in osmium tetroxide. Dehydration was in graded ethanol solutions and propylene oxide. Infiltration followed with a mixture of epoxy (Medcast; Ted Pella, Inc.) and propylene oxide and embedded in epoxy. One-μm sections were stained with azure II/methylene blue. Selected areas were thin sectioned, stained with urinal acetate and lead citrate, and examined with a Philips 410 electron microscope.

5-α Reductase Assay. Northern blot analysis for the 5α-reductase was kindly performed by the laboratory of Dr. Nicholas Bruchovsky (British Columbia Cancer Institute). Spe-

---

[4] E. Corey, manuscript in preparation.

Table 2 Tumor take rates in the human prostate cancer xenograft LuCaP 23

	LuCaP 23.1	LuCaP 23.8	LuCaP 23.12
Intact males	100% (10/10)[a]	90% (9/10)	67% (6/9)
Castrated males	40% (4/10)	50% (5/10)	20% (2/10)
Intact females	0% (0/10)	0% (0/10)	0% (0/10)

[a] Numbers in parentheses, number of successful tumor takes *vs.* number implanted.

cific cDNA probes for the 5α-reductase type 1 and 2 isoenzymes were hybridized to LuCaP 23 mRNA as described previously (23). Human BPH mRNA was used as a control.

Chromosomal Analysis. Chromosomal analysis was performed as a courtesy by Dr. Arthur Brothman (University of Utah).[5] Animals containing xenografts of LuCaP 23.1 passage 7 were sacrificed by cervical dislocation, and the entire tumor was excised. Tumor cells were mechanically dissociated and washed three times in HEPES-buffered saline (10 mM HEPES, 4 mM glucose, 3 mM KCl, 130 mM NaCl, and 1 mM Na_2HPO_4), and triplicate specimens were incubated at 37°C for 12 h, 36 h, and several days (in attempt to establish an *in vitro* culture) in RPMI 1640 supplemented with 10% fetal bovine serum (Life Technologies, Inc.). After the specified times, 0.01 μg/ml Colcemid was added for mitotic arrest, and specimens were G-banded as described previously (24). FISH using biotinylated probes for total human DNA (P5080; Oncor, Gaithersburg, MD), total mouse DNA (P2930; Oncor), and total human centromere DNA (P5095; Oncor) was performed on prepared cells using established procedures (25).

RESULTS

***In Vitro* Growth.** There was initial outgrowth of epithelioid cells in a confluent monolayer from tumor fragments harvested at autopsy. PSA was detected in conditioned media of the tissue culture flasks. Detection of PSA was lost after one to two passages, and cells became senescent shortly thereafter. Subsequently, numerous attempts were made to establish permanent cell lines from the established xenografts. Cells were cultured in two different growth medias, in addition to a variety of plate coatings, supplemented with growth factors and hormones. Cultures were established from the xenografts and behaved similar to cultures derived from the initial tumor fragments (*e.g.*, confluent monolayers of epithelioid cells with detectable PSA in the conditioned tissue culture media). However, similar to the primary cultures established from autopsy specimens, the cells became senescent after one to two passages. In Matrigel, cells formed spheroid colonies, and cell growth was maintained for up to 4 weeks, but continuous cultures were not attainable.

Establishment of the Xenografts. Tumor bits harvested from two separate retroperitoneal lymph nodes and a liver metastasis in the donor evolved into three xenograft sublines (designated LuCaP 23.1, 23.8, and 23.12, respectively), which
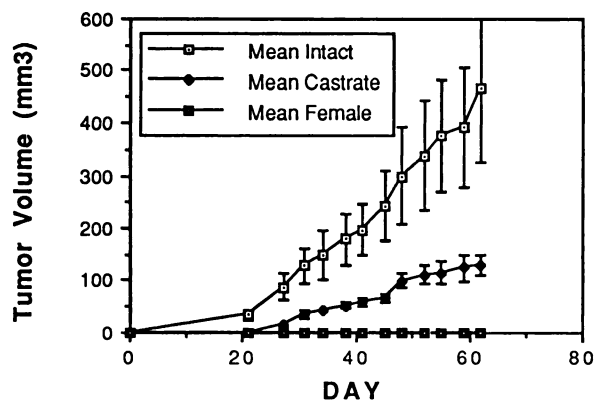
[5] B. J. Williams *et al.*, manuscript in preparation.

Fig. 2 An example of differential growth of the LuCaP 23 xenograft in intact male, castrated male, and intact female mice. Data shown are from the LuCaP 23.1 subline. Growth is slowed in the castrated mice, and no growth is observed in the female mice.

are serially transplantable and currently maintained in our animal facility. Growth of tumors was first detectable approximately 55 days postimplantation and confirmed by the presence of PSA and PAP in mouse serum. From the time of initial implantation of tumors in August 1991 until June 1995, the LuCaP 23.1, 23.8, and 23.12 xenografts have been passaged 17, 17, and 14 times, respectively. Xenografts are currently passaged approximately every 14 weeks. Once established as a transplantable xenograft, the growth rates have not changed.

***In Vivo* Growth.** Tumors arising from s.c. implantation of $20-25\text{-mm}^3$ tumor bits tumors are typically visible by days 30–45. Representative growth curves from the three sublines are shown in Fig. 1. Tumor doubling times for the LuCaP 23.1, 23.8, and 23.12 sublines are approximately 11, 15, and 21 days, respectively. In the three xenografts, tumor take rates are impaired in castrated male mice, and no tumors grow when implanted in female mice, as shown in Table 2. Tumor growth is also decreased in castrated animals (Fig. 2). Growth in castrated female mice is comparable to that in castrated male mice because tumor take rates and growth are similar (data not shown).

Determination of Serum PSA and PAP Concentrations. Production of PSA by the LuCaP 23 xenografts proceeds visible tumor growth by 1–3 weeks and is detectable in the serum approximately 14–28 days postimplantation. As shown in Fig. 2, serum PSA in intact male mice correlates with tumor volume in each xenograft ($r^2 = 0.6$, 0.8, and 0.8 respectively, in LuCaP 23.1, 23.8, and 23.12). The PSA index was 1.27, 1.63, and 5.21 ng/ml/mm^3, respectively, in LuCaP 23.1, 23.8, and 23.12 xenografts. Serum PAP concentrations are measurable in mice bearing the three LuCaP 23 xenograft sublines in a ratio to serum PSA concentrations of approximately 1:10. After surgical removal of the xenografts, the average serum PSA half-life was 12.9 ± 0.9 h ($r^2 = 0.9$). As previously described for the LNCaP mouse model, PSA clearance in that of LuCaP follows a two-compartment model of first-order elimination kinetics (18).

Castration-induced Effects. Castration-induced effects on serum PSA levels and tumor volume in the LuCaP 23.1 and 23.12 sublines are shown in Figs. 3 and 4. Individual mouse serum PSA levels and tumor volumes were normalized to the

A

B

Fig. 3 A, PSA response to castration (time 0) in the LuCaP 23.1 xenograft can be categorized into three groups: one group exhibits a prolonged response to castration (responders; △), a second group progresses between days 20 and 50 (partial responders; ■), and a third group exhibits minimal response to castration (●). B, tumor volume in the same animals from A. Animals are categorized by PSA response. Note that tumor volume is affected less by castration than serum PSA.
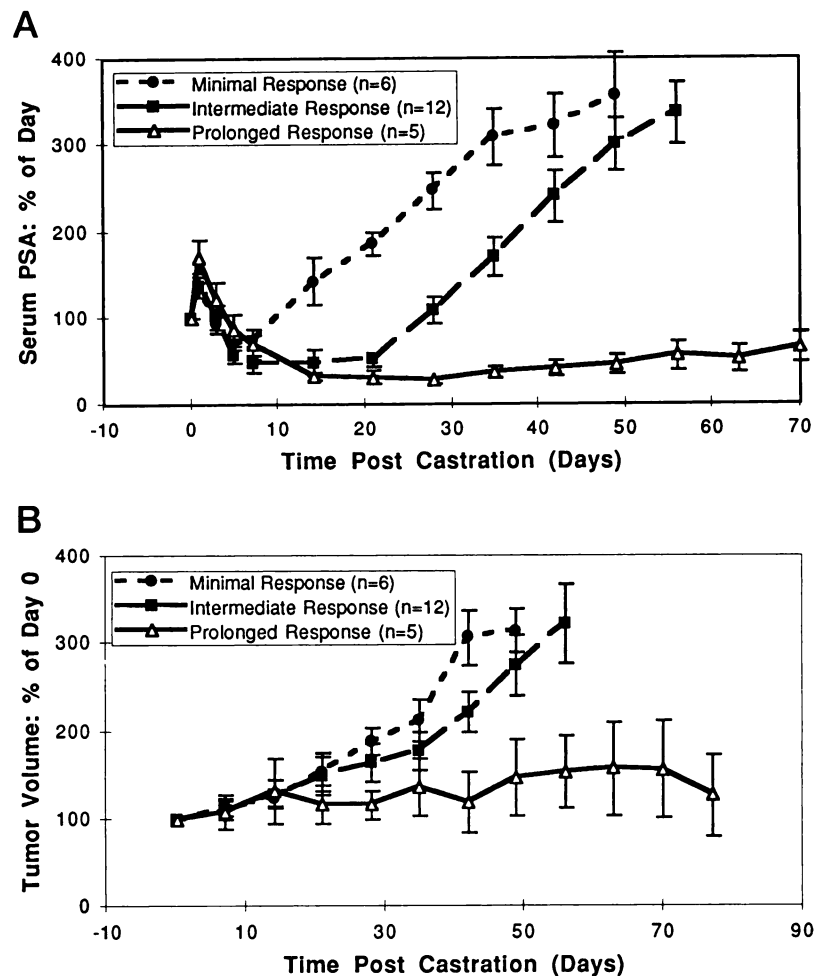
values measured at the time of castration. Tumors were assumed to be hormone refractory when PSA values exceeded those prior to castration for two subsequent measurements. Using this criteria, xenografts were classified into three groups according to their length of response to castration. The first group is characterized by a prolonged decrease (>50 days) in serum PSA levels after castration. The second group exhibits an intermediate response to castration (PSA decrease enduring 20–50 days postcastration). The final group of animals demonstrate a minimal decrease (<20 days) in PSA sera levels following castration. Based on these criteria, in the LuCaP 23.1 subline a prolonged response was noted in 5 (22%) of 23, an intermediate response was noted in 12 (52%) of 23, and a minimal response was noted in 6 (26%) of 23 animals after castration (Fig. 3). The LuCaP 23.12 subline exhibited a greater response to castration with 6 (50%) of 12 animals demonstrating a prolonged response, 3 (25%) of 12 animals demonstrating an intermediate response, and 3 (25%) of 12 animals demonstrating a minimal response to castration (Fig. 4).

Changes in tumor volume are usually smaller than changes in serum PSA. In general, those animals with the greatest response to castration by PSA criteria also show the greatest response by tumor volume criteria. The variability in response to

castration is independent of the source of the xenograft as tumors derived from the same parent xenograft produced heterogeneous responses to castration.

The decrease in serum PSA correlated with progression in the animals. As demonstrated in Table 3, those animals with the longest time to progression also exhibited the greatest decreases in serum PSA. These decreases in serum PSA were also continued for longer periods of time in the better-responding tumors as reflected in the time to reach PSA nadir.

Histology. Histological examination of the metastatic tumors harvested from the patient revealed sheets of cells with extensive necrosis. No clear gland formation was noted but the necrosis precluded adequate evaluation. Examination of the xenografts reveals a glandular pattern which resembled a Gleason's grade 3–4 adenocarcinoma, as shown in Fig. 5. The nuclei of the cells are pleomorphic with large nucleoli. The luminal cells exhibit a columnar morphology with polarity. Scattered neuroendocrine cells are visible. Occasional structures which appear to be apoptotic bodies are also present, which increase in number following castration. Little stroma is noted within the xenografts. Presumably, the stroma that is present is of mouse origin. Extensive necrosis and cystic areas are apparent within the larger xenografts.
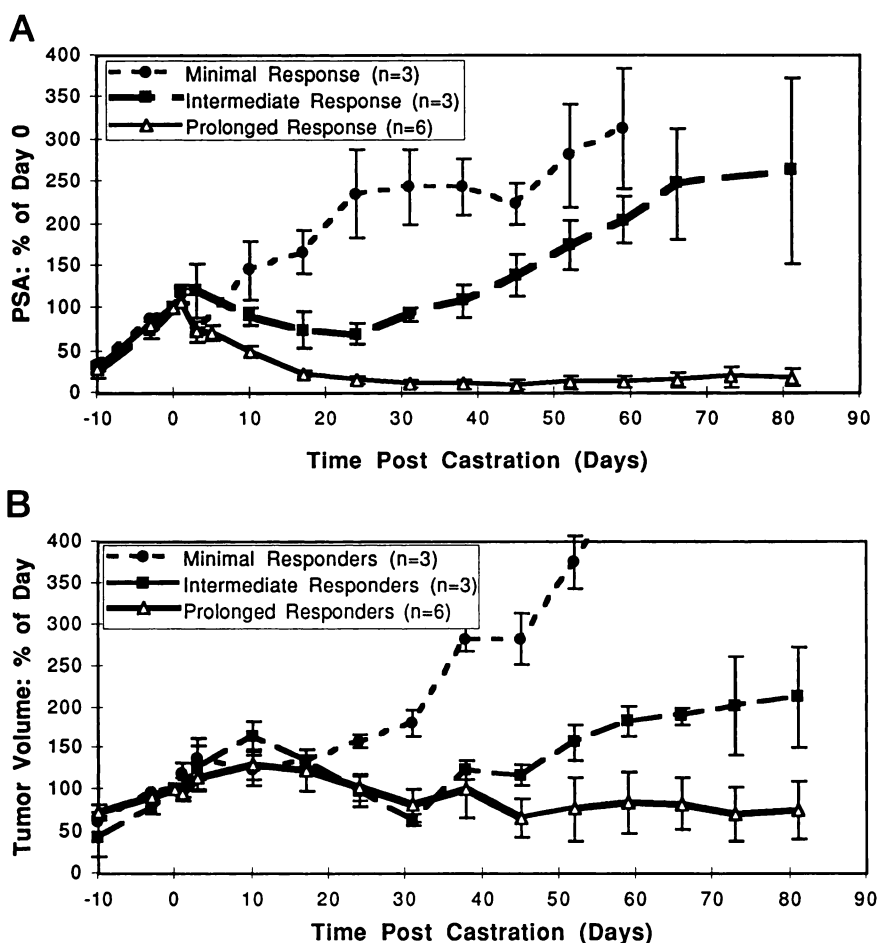
A

B

Fig. 4 A, LuCaP 23.12 xenografts subdivided into prolonged (>50 days; △), partial (between 20 and 50 days; ■), and minimal (<20 days; ●) response to castration. B, tumor volume responses to castration in the same animals from A. Animals are categorized by PSA response.

Table 3 Relationship between PSA response and tumor progression

|	Time to progression <50 days	Time to progression >50 days	P
LuCaP 23.1	n = 18	n = 5	
% PSA decrease	55.7 ± 6.5	82.2 ± 5.3	=0.05
Time to PSA nadir	10.9 ± 1.1	30.8 ± 10.0	<0.005
LuCaP 23.12	n = 6	n = 6	
% PSA decrease	35.5 ± 7.2	91.7 ± 4.6	<0.001
Time to PSA nadir	10.0 ± 3.6	55.7 ± 7.7	<0.001

Results of immunohistochemical studies are summarized in Table 4. PSA and PAP were consistently detected within the cytoplasm of all epithelial cells. An example of immunostaining with an anti-PSA antibody is demonstrated in Fig. 6. Monoclonal antibody 7E11-C5 reacted with at least 30% of the cells of LuCaP 23.1 but <10% of the cells within LuCaP 23.8 and 23.12. Monoclonal antibodies PD-41 and TURP-27 did not show appreciable reactivity in the different xenografts. The strongest staining against the epithelial cells of the three xenografts was obtained with the monoclonal antibody A6H. Immunostaining for the androgen receptor is shown in Fig. 7.

Immunostaining is localized to the tumor cell nuclei with a heterogeneous staining pattern.

Electron Microscopy. As shown in Fig. 8, LuCaP 23 cells exhibit nuclear polymorphism with prominent nucleoli and pseudoinclusions of cytoplasm in some nuclei when viewed with electron microscopy. Desmosomes and plasma membrane interdigitations are present on the cytoplasmic membrane between epithelioid cells surrounding the pseudoglandular lumen. Clusters of round to oval electron-dense structures, which range in diameter from 0.5 to 5 μm, are observed within the cytoplasm of tumor cells. These structures are ultrastructurally similar to secondary lysosomes which are abundant in normal and neoplastic prostate carcinoma.

5-α Reductase Assay. Northern blot analysis of mRNA extracted from the xenografts is shown in Fig. 9. The message for 5α-reductase type 1 is present in the xenografts, whereas the message for 5α-reductase type 2 is not detected. Both type 1 and type 2 transcripts are detectable in control BPH mRNA.

Chromosomal Analysis. Metaphase preparations were of poor quality, and the mitotic index was low for all specimens. The most satisfactory mitotic values were obtained following the 12-h incubation; long-term *in vitro* cultures could not be established. A total of 48 metaphases were evaluated following G-banding with Wright stain. The chromosome number ranged
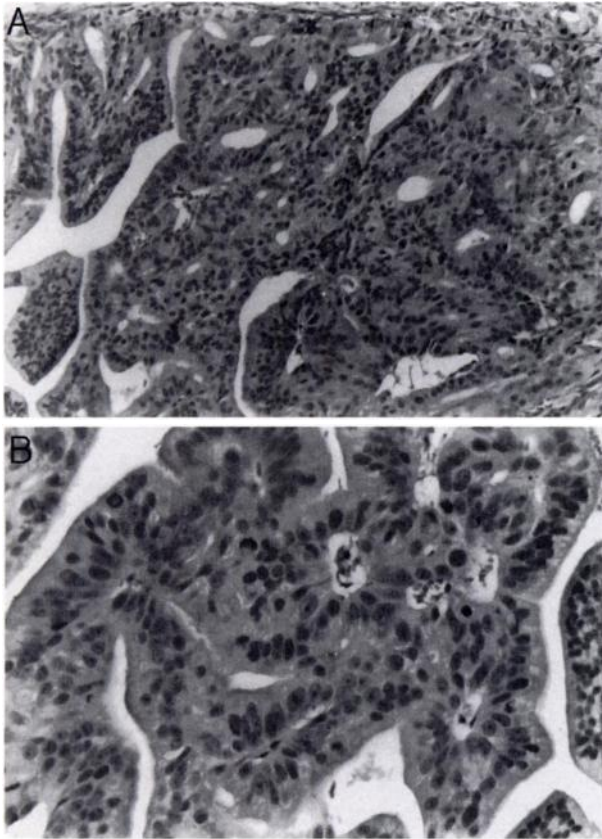
Fig. 5   A, photomicrograph of a representative portion of a H&E-stained section of tumor. The tumor is composed of glands that have lumina of various sizes and shapes and that grow back-to-back with adjacent tumor glands. B, higher magnification photomicrograph of tumor demonstrates glandular lumina lined by dysplastic tumor cells that have nuclei basally oriented away from the lumina.

from 62 to 112 chromosomes/cell, with a modal number of 78. Multiple structural and numerical abnormalities were detected, and many normal human chromosomes could be identified, but a definitive karyotype could not be prepared due to poor morphology. FISH analysis of both metaphase and interphase nuclei using the total human DNA showed diffuse signal, whereas the total mouse DNA showed no signal (a positive control using mouse cells showed signal with this probe). Total human centromere DNA showed strong, distinct signals.

DISCUSSION

In this article, we describe a new prostate cancer xenograft system, LuCaP 23, which retains two of the clinical hallmarks of prostate carcinoma, androgen responsiveness and PSA production. Three different sublines were developed from three different metastases harvested from the tumor donor shortly after death. LuCaP 23.1 and 23.8 were developed from lymph node metastases, while LuCaP 23.12 was developed from a liver metastasis.

The LuCaP 23 series of xenografts were generated from metastases in a patient with end stage hormone-resistant prostate cancer. Xenografts derived from such a patient would be ex-

pected to exhibit androgen-independent behavior. However, these tumors clearly are androgen sensitive, and many of the tumors appear to be androgen dependent as demonstrated by a marked decrease in serum PSA levels and a lesser, but demonstrable, decrease in tumor size following castration. Investigators have described variable responses to castration in the most commonly studied xenograft system, LNCaP. Lim et al. (26) reported tumor involution in response to androgen withdrawal in LNCaP xenografts. On the other hand, Gleave et al. (27) reported tumor size stabilizes, or may even increase, following castration. In our experience with LNCaP xenografts, the tumors do not decrease in size following castration.[6] In the PC-82 xenograft, Kyprianou et al. (28) reported that programmed cell death and tumor involution occur in response to androgen withdrawal.

Androgenic effects in the human prostate are primarily regulated by the interaction of DHT with the androgen receptor. Androgen receptor is present in most of the LuCaP 23 cell nuclei as determined using immunostaining. Whether or not there are mutations of this androgen receptor is not yet known. DHT is produced from testosterone by the enzyme 5 α-reductase. The heterogeneity in androgen responsiveness could be related to heterogeneity in the androgen receptor staining. The predominant isozyme of 5 α-reductase present in the prostate is type 2 (29). Interestingly, this isozyme is present in the prostatic stromal cells, not in the epithelial cells. Prostate epithelial cells produce the type 1 isozyme of 5-α-reductase, which is also present in the skin (30). The presence of the type 1 isozyme in these xenografts is consistent with the prostatic epithelial origin of these tumors.

The production of PSA is an important characteristic of prostate carcinomas and a desirable characteristic of prostate cancer models. PSA is a M_r 34,000 serine protease produced by benign and malignant prostate epithelial cells, which is reviewed elsewhere (31). This enzyme is responsible for liquefaction of the seminal coagulum (32). The discovery that serum PSA levels can be elevated by prostatic neoplasms has made PSA one of the most valuable tumor markers in all of oncology. PSA has replaced bone scans and acid phosphatase determinations as the primary means of monitoring disease status in patients with prostate cancer. Responses to therapy are commonly described in terms of changes in PSA levels. The production of PSA by prostate cancer xenografts is an important characteristic which confirms prostatic origin of the tumor, suggests the model will behave in a fashion similar to human prostate cancer, and allows the modeling of clinical scenarios. Serum PSA levels in mice bearing the LuCaP 23 xenografts correlate with tumor growth. Following androgen ablation, the decrease in PSA as well as the time to reach PSA nadir correlate with time to tumor progression. Both of these observations model the findings in clinical prostate cancer. The expression of this marker allows the investigator to monitor tumor burden when the tumors are not easily measurable (i.e., subrenal capsule implantation, orthotopic prostate implantation, extremely small tumors, or metastatic disease). The PSA production by LuCaP 23 is many fold higher

---

[6] Unpublished data.

Table 4 Results of immunohistochemical staining of the LuCaP 23 sublines

Monoclonal antibodies	LuCaP 23.1		LuCaP 23.8		LuCaP 23.12	
	Staining[a] intensity	% Positive[b] cells	Staining intensity	% Positive cells	Staining intensity	% Positive cells
Anti-PAP	2–3+	100	2–3+	100	2–3+	100
Anti-PSA						
16–3A2	3–4+	100	3–4+	100	3–4+	100
22–8A2	3–4+	100	3–4+	100	3–4+	100
Antirenal cancer and prostate cancer						
A6H	4+	100	4+	100	4+	100
Antiprostate carcinoma						
7E11-C5	2–3+	30	1–2+	SC[b]	0	
PD-41	2–3+	SC	0		2–3+	1
TURP-27	2–3+	SC	3–4+	SC	2–3+	SC

[a] 0, no staining; 1+, weak staining; 2+, moderate staining; 3+, strong staining; 4+, very strong staining.
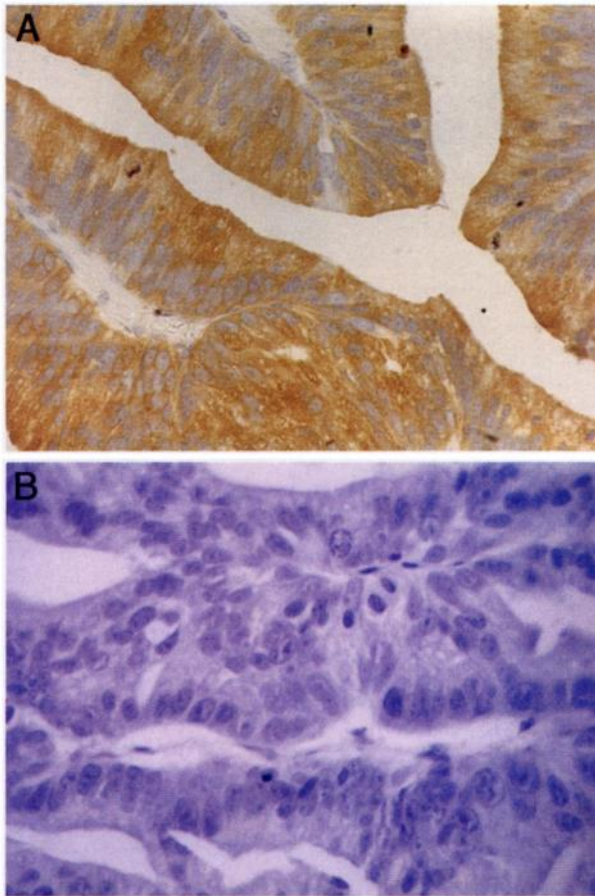[b] SC, scattered cells.

Fig. 6 A, immunohistochemical staining with anti-PSA monoclonal antibodies. The cells polarized with intense apical cytoplasmic reactivity with the anti-PSA antibodies. B, MOPC control.

Fig. 7 High magnification of tumor immunostained for androgen receptor. Immunoreactivity is localized exclusively in the tumor epithelial cell nuclei.

than that by any of the other prostate cancer xenografts which are known to produce measurable serum PSA levels.

Because *in vitro* cultures could not be established, detailed classical cytogenetic analysis could not be performed. The preparations were 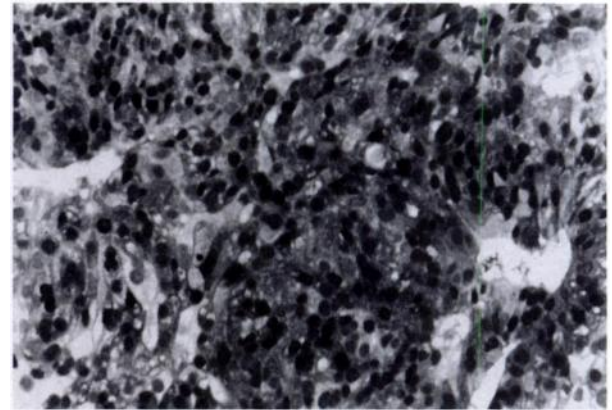acceptable, however, to determine the human origin of LuCaP 23.1 by G-banding, and a hypertriploid to near-tetraploid karyotype was observed. FISH proved to be a valuable technique for confirmation of these findings, using total human and total mouse probes. There was no evidence of any mouse cells in the harvested material evaluated. A more detailed molecular cytogenetic characterization of these cells is ongoing and will be presented elsewhere.

The reason for the relative lack of expression of PD41, TURP-27, and 7E11-C5 is unclear. PD-41 is an important antigen which appears to react with most (65%) human prostatic carcinomas (20). The TURP-27 antigen is expressed to various degrees by both benign and malignant prostatic tissue (33). The 7E11-C5 antibody was developed by Horoszewicz *et al.* (22) to an antigen in the prostate cancer cell membrane. The antibody is used experimentally in radioimmunoscintigraphy and radioimmunotherapy. One of the most interesting aspects of 7E11-C5 is that while it is expressed in most prostate cancer cells, overexpression occurs in those tumors exhibiting hormone independence (34). In the LuCaP 23 series, <30% of the cells exhibit 7E11-C5 reactivity. It is not known whether these cells represent a hormonally independent subset of the tumor cells.

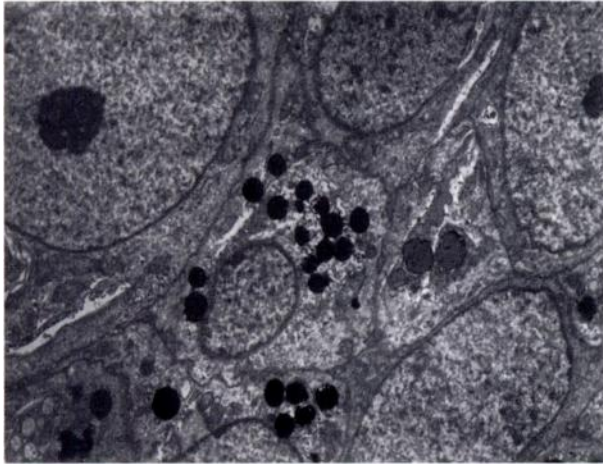Although the characteristics of the three LuCaP 23 sublines

Fig. 8 Electron micrograph of LuCaP 23.1 xenograft. Many of the nuclei contain large nucleoli. Numerous electron-dense granules of uncertain origin are present within the cytoplasm of the cells. ×3000.
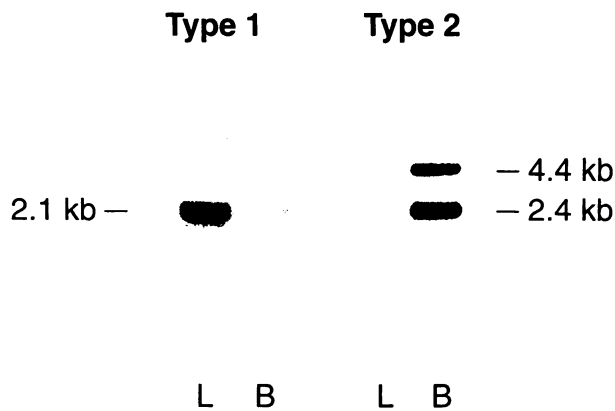

Fig. 9 Northern blot hybridization of LuCaP 23 (*L*) and human BPH (*B*) mRNA with 5α-reductase type 1 (*left panel*) and type 2 (*right panel*)-specific cDNA. The 5α-reductase type 1 cDNA hybridizes to a 2.1-kb transcript visible in both the LuCaP 23 and the BPH mRNA. The 5α-reductase type 2 cDNA hybridizes to a 2.4- and 4.4-kb transcript visible only in the BPH lanes.

described in this article are similar, there are apparent differences in doubling time, PSA production, and hormonal responsiveness. LuCaP 23.12 appears to be the most differentiated of the tumors by virtue of a slower growth rate, higher PSA production, and greater response to androgen deprivation. These differences are to be expected given the heterogeneous nature of tumors and metastases. This tumor heterogeneity appears to extend to the individual xenograft since multiple explants of a single xenograft are noted to have differing responses to castration. In contrast, xenografts derived from cell lines tend to be more homogeneous in their behavior because each animal is inoculated with a cell population representative of the uniform cell culture population. Although heterogeneous xenografts are more difficult to study, they nonetheless represent the complexities of clinical prostatic carcinoma, which is a multifocal dis-

ease with different cytogenetic markers expressed by different tumor foci. This heterogeneity is reflected in the heterogeneous response to therapy in human prostate carcinoma.

To date, we have been unsuccessful in immortalizing these cells in tissue culture. The development of such a cell line is important because it allows study of questions that cannot be answered in the xenograft model. However, if heterogeneity is as important as we believe, the transfer from xenograft to cell line and back to xenograft may result in an inferior model due to the homogeneity of the new tumor. Similarly, immortalization of the cells by viral transfection might change the characteristics of this model. Nonetheless, such efforts are under consideration.

We believe this new human prostate cancer xenograft system will provide valuable insight into the biology of prostate carcinoma. This model has the desirable characteristics of PSA production, hormonal responsiveness, and a relatively rapid growth rate. Our hope is that these characteristics will allow study of the changes associated with the progression from an androgen-dependent to an androgen-independent tumor.

REFERENCES

1. Boring, C. C., Squires, T. S., and Tong, T. Cancer statistics, 1993. CA Cancer J. Clin., *43:* 7–26, 1993.

2. Okada, K., and Schroeder, F. Human prostatic carcinoma in cell culture: preliminary report on the development and characterization of an epithelial cell line. Urol. Res., *2:* 111–121, 1974.

3. Stone, K. R., Mickey, D. D., Wunderli, H., Michey, G. H., and Paulson, D. F. Isolation of a human prostate carcinoma cell line (DU-145). Intl. J. Cancer, *21:* 274–281, 1978.

4. Kaighn, M., Shakar Narayan, K., Ohnuki, Y., Lechner, J., and Jones, L. Establishment and characterization of a human prostatic carcinoma cell line (PC-3). Urology, *17:* 16–23, 1979.

5. Horoszewicz, J. S., Leong, S. S., Chu, T. M., Wajsman, Z. L., Freedman, M., Papsidero, L., Kim, U., Chai, L. S., Kakati, S., Arya, S. K., and Sandberg, A. A. The LnCaP cell line—a new model for studies on human prostatic carcinoma. Prog. Clin. Biol. Res., *37:* 115–132, 1980.

6. Class, F., and Van Steenbrugge, G. J. Expression of HLA-like structures on a permanent human tumor line PC-93. Tissue Antigens, *21:* 227–232, 1983.

7. Iizumi, T., Yazaki, T., Kanoh, S., Kondo, I., and Koiso, K. Establishment of a new prostatic carcinoma cell line (TSU-PR1). J. Urol., *137:* 1304–1306, 1987.

8. Muraki, J., Addonizio, J., Choudhury, M., Fischer, J., Eshghi, M., Davidian, M., Sharppiro, L., Wilmot, P., Nagamatsu, G., and Chiao, J. Establishment of new human prostatic cancer cell (JCA-1). Invest. Urol., *36:* 79–84, 1990.

9. Gingrich, J., Tucker, J., Walther, P., Day, J., Poulton, S., and Webb, K. Establishment and characterization of a new human prostatic carcinoma cell line (DuPro-1). J. Urol., *146:* 915–919, 1991.

10. Narayan, P., and Dahiya, R. Establishment and characterization of a human primary prostatic adenocarcinoma line (ND-1). J. Urol., *148:* 1600–1604, 1992.

11. Hoehn, W., Schoroeder, F. H., Riemann, J. F., Joebsis, A. C., and Hermanek, P. Human prostatic adenocarcinoma: some characteristics of a serially transplantable line in nude mice (PC 82). Prostate, *1:* 95–104, 1980.

12. Ito, Y. Z., Mashimo, S., Nakazato, Y., and Takikawa, H. Hormone dependency of a serially transplantable human prostatic cancer (HONDA) in nude mice. Cancer Res., *45:* 5058–5063, 1985.

13. Graham, S. D., Poulton, S. H., Linder, J., Woodard, B. H., Lyles, K. W., and Paulson, D. F. Establishment of a long-term adenocarcinoma of the prostate cell line in the nude mouse. Prostate, *7:* 369–376, 1985.

14. Hoehn, W., Wagner, M., Riemann, J. F., Hermanek, P., Williams, E., Walther, R., and Schruffer, R. Prostatic adenocarcinoma PC-EW, a new human tumor line transplantable in nude mice. Prostate, 5: 445–452, 1984.

15. Van Steenbrugge, G., Groen, M., Bolt-de Vries, J., Romijn, J., and Schroeder, F. Human prostate cancer (PC-82) in nude mice: a model to study androgen regulated tumor growth. Prog. Clin. Biol. Res., 185A: 23–50, 1985.

16. Caspo, Z., Brand, K., Walther, R., and Konstantinos, F. Comparative experimental study of the serum prostate specific antigen and prostate acid phosphatase in serially transplantable human prostatic carcinoma lines in nude mice. J. Urol., 140: 1032–1038, 1988.

17. Harper, M., Sibley, P., Rowlands, A., Buttifant, L., Beacock, C., and Griffiths, K. Hormonal modulation of the growth of a new transplantable prostatic cell line in athymic mice. Urol. Res., 14: 156A, 1986.

18. Gleave, M. E., Hsieh, J. T., Wu, H., Von Eschenbach, A. C., and Chung, L. W. Evaluation of the pharmacokinetics of PSA using the LNCaP tumor model. J. Urol., 147: 694, 1992.

19. Gleason, D. F. Histologic grading in clinical staging of prostatic carcinoma. In: M. Tannenbaum (ed.), Urologic Pathology: The Prostate, pp. 171–179. Philadelphia: Lea & Febiger, 1977.

20. Beckett, M. L., Lipford, G. B., Haley, C. L., Schellhammer, P. E., Wright, G. L., Jr. Monoclonal antibody PD41 recognizes an antigen restricted to prostate adenocarcinomas. Cancer Res., 51: 1326–1333, 1991.

21. Starling, J. J., Sieg, S. M., Beckett, M. L., Wirth, P. R., Wahab, Z., Schellhammer, P. F., Ladaga, L. E., Ploeskic, S., and Wright, G. L., Jr. Human prostate tissue antigens defined by murine monoclonal antibodies. Cancer Res., 46: 367–374, 1986.

22. Horoszewicz, J. S., Kawinski, E., and Murphy, G. P. Monoclonal antibodies to new antigenic marker in epithelial prostatic cells and serum of prostatic cancer patients. Anticancer Res., 7: 927–936, 1987.

23. Kaefer, M., Audia, J., Bruchovsky, N., Goode, R., Hsiao, K., Libovitch, I., Kruchinsky, J., Lee, C., Steidle, C., Sutowski, D., and Neubauer, B. Characterization of type I 5-alpha reductase activity in DU145 human prostatic adenocarcinoma cells. J. Steroid Biochem. Mol. Biol., in press, 1996.

24. Brothman, A. R., Peeh, D. M., Patel, A. M., and McNeal, J. E. Frequency and pattern of karyotypic abnormalities in human prostate cancer. Cancer Res., 50: 3795–3803, 1990.

25. Brothman, A., Patel, A., Peehl, D., and Schellhammer, P. Analysis of prostatic tumor cultures using fluorescence in situ hybridization (FISH). Cancer Genet. Cytogenet., 62: 180–185, 1992.

26. Lim, D. J., Liu, X. L., Sutkowski, D. M., E. J. B., Lee, C., Kozlowski, J. M. Growth of an androgen-sensitive human prostate cancer cell line, LNCaP, in nude mice. Prostate, 22: 109–118, 1993.

27. Gleave, M. E., Hsieh, J. T., Wu, H. C., von Exchenbach, A. C., and Chung, L. W. K. Serum prostate specific antigen levels in mice bearing human prostate LNCaP tumors are determined by tumor volume and endocrine and growth factors. Cancer Res., 52: 1598–1605, 1992.

28. Kyprianou, N., English, H., and Isaacs, J. Programmed cell death during regression of PC-82 human prostate cancer following androgen ablation. Cancer Res., 50: 3748–3753, 1990.

29. Thigpen, A. E., Silver, R. I., Guileyardo, J. M., Casey, M. L., McConnell, J. D., and Russell, D. W. Tissue distribution and ontogeny of steroid 5 alpha-reductase isoenzyme expression. J. Clin. Invest., 92: 903–910, 1993.

30. Harris, G., Azzolina, B., Baginsky, W., Cimis, G., Rasmusson, G. H., Tolman, R. L., Raetz, C. R. H., and Ellsworth, K. Identification and selective inhibition of an isozyme of steroid 5 alpha-reductase in human scalp. Proc. Natl. Acad. Sci. USA, 89: 10787–10791, 1992.

31. Ellis, W. J., and Brawer, M. K. The role of tumor markers in the diagnosis and treatment of prostate cancer. In: H. Lepor and R. K. Lawson (eds.), Prostate Diseases, pp. 276–291. Philadelphia: W. B. Saunders Company, 1993.

32. Lilja, H. A kallikrein-like serine protease in prostatic fluid cleaves the predominant seminal vesicle protein. J. Clin. Invest., 76: 1899–1903, 1985.

33. Wright, G. L., Jr., Beckett, M. L., Lipford, G. B., Haley, C. L., and Schellhammer, P. F. A novel prostate carcinoma-associated glycoprotein complex (PAC) recognized by monoclonal antibody Turp-27. Int. J. Cancer, 47: 717–725, 1991.

34. Israeli, R. S., Powell, C. T., Corr, J. G., Fair, W. R., and Heston, W. D. W. Expression of the prostate-specific membrane antigen. Cancer Res., 54: 1807–1811, 1994.